Saudi Journal of Biological Sciences 27 (2020) 3700–3710

Contents lists available at ScienceDirect

Saudi Journal of Biological Sciences

journal homepage: www.sciencedirect.com

Original article

Thunbergia laurifolia leaf extract partially recovers lead-induced renotoxicity through modulating the cell signaling pathways

Mohammad Nasiruddin Rana [a,b,d], Naymul Karim [a,d], Suksan Changlek [a,d], Md. Atiar Rahman [c], Jitbanjong Tangpong [a,d,*], Dina Hajjar [e], Walla Alelwani [e], Arwa A. Makki [e]

[a] *Biomedical Sciences, School of Allied Health Sciences, Walailak University, Nakhon Si Thammarat 80161, Thailand*
[b] *Department of Pharmacology, Zhejiang University School of Medicine, Hangzhou 310058, PR China*
[c] *Department of Biochemistry and Molecular Biology, University of Chittagong, Chittagong, Bangladesh*
[d] *Research Excellence Center for Innovation and Health Products (RECIHP), Walailak University, Nakhon Si Thammarat 80160, Thailand*
[e] *Department of Biochemistry, College of Sciences, University of Jeddah, Jeddah 80203, Saudi Arabia*

ARTICLE INFO

Article history:
Received 3 May 2020
Revised 4 August 2020
Accepted 9 August 2020
Available online 13 August 2020

Keywords:
Thunbergia laurifolia Linn.
Lead (Pb)
Oxidative stress
Anti-inflammation
Renotoxicity

ABSTRACT

This research investigated the reno-protective effect of *Thunbergia laurifolia* Linn. (TL) in a lead-induced toxicity test through the modulation of cell signaling pathways. The study carried out to evaluate the effect of TL leaf extracts in Swiss Albino mice exposed to lead acetate (PbAc). Prior to *in vivo* study, a probable kidney-protective effect of the plant leaf extract was presumed through an activity-specific (PASS) molecular docking analysis. In animal model study, albino mice were divided in seven groups and co-treated with PbAc and TL (100, 200 mg/kgBW) or vitamin E (100 mg/kgBW) for 38 days, whereas the untreated control, TL control, and vehicle control groups received sodium acetate, PbAc, sodium acetate plus mineral oil, respectively. At the end of treatment, blood and kidney tissue were collected for investigating Pb concentration, estimating biochemical profile, evaluating oxidative stress and inflammatory parameters. The histopathological change of kidney along with apoptosis was assessed from kidney sections using H & E staining and TUNEL assay. Pb-exposed mice were found to be increased concentration of Pb in the blood and kidney sample, which further led to increased MDA levels in the plasma, blood, and tissue. Followed by kidney damage, increased expression of TNF-α, iNOS, and COX-2 in kidney tissues were noticed, which were related to elevated TNF-α in the systemic circulation of Pb-treated mice. Co-treatment with TL or vitamin E significantly reduced altered structure and apoptosis of kidney tissues. Downregulation of inflammatory markers especially TNF-α, iNOS, and COX-2 with simultaneous improvement of renal function through reduced plasma BUN and creatinine levels demonstrate that TL act as a potential dietary supplement to detoxify Pb in kidney showing an antioxidant and anti-inflammatory effect.
© 2020 Published by Elsevier B.V. on behalf of King Saud University. This is an open access article under the CC BY-NC-ND license (http://creativecommons.org/licenses/by-nc-nd/4.0/).

1. Introduction

Lead (Pb) poisoning is an occupational health hazard especially in the third world and industrializing countries (Azeh Engwa et al., 2019). Widespread usage of Pb in different industries including automobiles, paints, ceramics, plastics, and similar industries makes its abundance in the environment to cause environmental pollution (Centers for Disease control and Prevention, 2020). It can exist for a long time in gasoline, industrial processes such as Pb smelting coal combustion, Pb-based paints, Pb containing pipes, battery recycling, grids, and bearings due to its non-degradability. Intoxication with Pb followed by deposition in the body is related to different diseases such as neurotoxicity or neurodegenerative diseases, immunological disorders, gastrointestinal diseases, hematological diseases, and reproductive complexity, etc.

Abbreviations: Pb, lead; ROS, reactive oxygen species; DNA, Deoxyribonucleic acid; TL, *Thunbergia laurifolia* Linn.; BW, body weight; TNF-α, Tumor necrosis factor-alpha; iNOS, Inducible nitric oxide synthase; COX-2, Cyclooxygenase-2; ELISA, enzyme-linked immunosorbent assay; MDA, Malondialdehyde; BUN, Blood urea nitrogen; GFR, Glomerular filtration rate; TBARS, Thiobarbituric acid reactive substances; TBST, Tris phosphate buffer saline with Tween 20; TBS, Tris phosphate saline; H&E, Hematoxylin-Eosin; TUNEL, Terminal deoxynucleotidyl transferase dUTP nick end labeling.

* Corresponding author at: School of Allied Health Sciences, Walailak University, Nakhon-Si-Thammarat 80160, Thailand.
E-mail address: rjitbanj@wu.ac.th (J. Tangpong).

Peer review under responsibility of King Saud University.

Production and hosting by Elsevier

https://doi.org/10.1016/j.sjbs.2020.08.016
1319-562X/© 2020 Published by Elsevier B.V. on behalf of King Saud University.
This is an open access article under the CC BY-NC-ND license (http://creativecommons.org/licenses/by-nc-nd/4.0/).

(Ademuyiwa et al., 2007; Patrick, 2006; Tangpong and Satarug, 2010; Vega-Dienstmaier et al., 2006) and kidney is the second most vulnerable for Pb toxicity after the brain (Orr and Bridges, 2017). This Pb toxicity is documented to be linked with oxidative stress, the key mechanism of Pb toxicity, which is connected with enhanced lipid peroxidation, reduced antioxidant activity, and kidney dysfunction (Rana et al., 2020, 2018). Moreover, the hindrance of cytosolic Ca^{2+} also evidenced with Pb-induced kidney toxicity (Rana et al., 2018). Chelating therapy is implemented in severe cases of Pb toxicity to hasten the elimination process of Pb deposition. However, several adverse effects such as transient leucopenia, hypotension, transient thrombocytopenia, rash, enuresis, Zn deficiency, and cellular redistribution of Pb etc. limit the success of chelating therapy (Lowry, 2010). Therefore, the development of therapeutics from alternative sources could meet the existing demand to overcome the Pb-associated health complexity.

Thunbergia laurifloia Linn. (TL, Acanthaceae) is a trumpet vine, widely distributed in Southeast Asian countries and native to India (Kanchanapoom et al., 2002). Antidote properties of TL have made it well known in Thailand, where dried leaves, dried roots, fresh leaves, and bark are used as traditional medicine (Rocejanasaroj et al., 2014). An earlier study reported that TL is active against pesticides, arsenic, and strychnine toxicity (P. Tejasen and Thongthapp, 1980). Moreover, a study from our lab unveiled that TL is effective against the cognitive dysfunction of mice with Pb exposed (Phyu and Tangpong, 2013). Tangpong and Satarug 2010 reported that TL act as a chelating agent against neuronal cell death and memory loss in Pb exposed mice (Tangpong and Satarug, 2010). According to the accumulated evidences, TL also possesses a wide range of pharmacological properties, for example, anti-mutagenic, anti-inflammatory and antipyretic properties along with antioxidant, anti-inflammatory, antimicrobial, neuroprotective, anti-proliferative, hepatoprotective, and antidiabetic activity (Chan et al., 2011; Tangpong and Satarug, 2010; Wonkchalee et al., 2012). Furthermore, it is also used in the treatment of drug addiction (Chan et al., 2011).

Currently, there is no existing study and insight mechanisms of TL effect against Pb induced kidney toxicity in the mice model. Thus, this study was designed to investigate the role of TL against lead acetate (PbAc) induced renal toxicity and its underlying mechanism.

2. Materials and methods

2.1. In silico study

2.1.1. Prediction of activity spectra (PASS) analysis

To predict the probable kidney protective effect of TL, a well-known computer-aided tool called "prediction of activity-specific for substances or PASS" program was used. PASS can predict a wide spectrum of biological activity based on the structural formula of the organic substances. The 2D structure (SDF file) of identified phytochemical constituents of TL leaves (Junsi and Siripongvutikorn, 2016) such as α-Spinosterol (PubChem CID 5281331), β-Sitosterol (PubChem CID 222284), Caffeic acid (PubChem CID 689043), Protocatechuic acid (PubChem CID 72), Gallic acid (PubChem CID 370), Apigenin (PubChem CID: 5280443), Grandifloric acid (PubChem CID: 159930), Lutein (PubChem CID: 5281243), 3'-O-β-glucopyranosyl-stilbericoside (PubChem CID: 6325264), Stigmasterol (PubChem CID: 5280794), Benzyl β-glucopyranoside (PubChem CID: 11076492), 6-C-glucopyranosyl apigenin (PubChem CID: 442658), 6,8-di-C-glucopyranosyl apigenin (PubChem CID: 3084407), 3-Hexenyl-beta-glucopyranoside (PubChem CID: 5318046), Hexanol beta-D-glucopyranoside (PubChem CID: 6428285) were uploaded in PASS online (way2drug). The output of probable activity was presented as Pa (active) and Pi (inactive). The output of probable activity was presented as Pa (active) and Pi (inactive) (Filimonov et al., 2014). Here, Pa > Pi was considered to be an active compound and Pa greater than 0.3 were believed to be experimentally effective.

2.1.2. Molecular docking study

To predict the insight of the protective mechanism, binding efficiency of phytoconstituent to IP3R receptor (PDB:3UJ0) that contributes to [Ca^{2+}] dysregulation (Wang et al., 2015), to activate Nrf-2 following release from KEAP1 (PDB:5CGJ) during oxidative stress were studied. Besides, the interaction among phytoconstituents and inflammatory mediators including TNF-α (PDB: 2AZ5), iNOS (PDB: 3E67), COX-2 (PDB: 5KIR), and proteins of MAPK pathways P38 Kinase (PDB: 2YIS), JNK (PDB: 3OY1), and NF-kB activity regulator, IκB kinase-β (PDB: 4KIK) were screened. Published crystal structures of aforementioned protein as PDB format were imported into Mastro software (Scodinger suit v11). To process the proteins for docking study, proteins preparation wizards were allowed to preprocess to add bond order, hydrogen bond, and create disulfide bond (Wright et al., 2020). Afterward, the minimization was carried out by applying the OPLS5 force field and 0.30 Å was set for the maximum heavy atom root-mean-square-deviation (RMSD).

To process the ligand, 2D structures of water soluble phytoconstituents, such as Caffeic acid (PubChem CID 689043), Protocatechuic acid (PubChem CID 72), Gallic acid (PubChem CID 370), were converted to 3D structure using the ligprep wizards (Scodinger suit v11) with a default setting of OPLS5 force field (pH 7.0 ± 2.0, allow 32 stereoisomers per ligand). After that, prepared proteins were processed to receptor grid generation by applying OPLS5 force field, and the ligands were allowed to dock flexibly using the ligand docking module. The resultant scores were extracted as an excel file, and the lowest docking score was considered as the best docking.

The drug likeliness properties of docked phytoconstituents were analyzed by the QikProp module of Schrodinger. Briefly, the 3D structures processed during the ligand preparation were input into QikProp wizard and then analyzed with the default setting. A compound was considered to possess characteristics resembles the available drug, if it met any three parameters out of four. The parameters were molecular weight < 500, hydrogen bond donor $\leq$ 5, hydrogen bond acceptor $\leq$ 10, and predicted octanol/water partition coefficient (QPlogPo/w) value (−)2.0 – 6.5.

2.2. In vivo study

2.2.1. Preparation of TL leaves extract

TL leaves (10 kg) were collected from Nakhon Si Thammarat, Thailand, during the month between April to May, and was identified by an expert botanist. A voucher specimen of the sample has been preserved in the University Herbarium with the accession number BKF 186138. The leaves were oven-dried at 60 °C for 4 h. Dried leaves were pulverized (Philip, Germany), soaked into water and autoclaved at 121 °C for 15 min. Afterward, the suspension was kept in dark at 4 °C for 2 days, filtered using Whatman No. 1, and then centrifuged at 4000 rpm for 15 min. The supernatant was collected and was kept at −40 °C for 12 h before lyophilization (EYELA, Tokyo, Japan). The yield value of TL extract was 9.65% in powder form and stored at −30 °C for further use.

2.2.2. Animals and experimental design

Forty eight-week-old ICR male mice (30–33 g) were purchased from National Laboratory Animal Center, Salaya district, Nakhon Pathom, Thailand. These mice were housed at polypropylene cages in the animal center of Walailak University, Thailand. The mice

were allowed to access standard food and water *ad libitum* for 2 weeks followed by standard laboratory conditions such as temperature (23 ± 2 °C), humidity (50 ± 5%), and light/dark cycle 12 h. To evaluate the effect of TL against Pb-induced nephropathy, mice were treated according to Phyu and Tangpong 2013, where Pb significantly impaired cognitive behavior and oral administration of TL extracts markedly improved cognitive function (Phyu and Tangpong, 2013). In this study, the experiments were randomly divided into seven independent groups (n = 6) and were continued for 38 days. The treatments strategies in different groups were as follows:

Group 1: Untreated Control, (received only 1% CH_3COONa in drinking water).
Group 2: PbAc (1% in DW) (received only 1% PbAc in drinking water).
Group 3: TL 200 mg/kgBW (received only 200 mg/kgBW of TL water extract; P.O.).
Group 4: Pb + TL 100 mg/kgBW (received 1% PbAc in drinking water + 100 mg/kgBW of TL water extract; P.O.).
Group 5: Pb + TL 200 mg/kgBW (received 1% PbAc in drinking water + 200 mg/kgBW of TL water extract; P.O.).
Group 6: Pb + Vit-E 100 mg/kgBW (received 1% PbAc in drinking water + 200 mg/kgBW of Vit-E in mineral oil, P.O.).
Group 7: Vehicle Control (received mineral oil, P.O).

Here, P.O (Per os) dictates the oral administration by gavage.

2.2.3. Sample collection

The mice were anesthetized using Nembutal sodium (65 mg/kg BW) and sacrificed via left ventricle puncture. Blood was obtained and then collected in a 2.5 mL K_3EDTA containing tube. Afterward, a portion of the right kidney was removed and homogenizes (Sonics VCX70, USA) in a mixture of cold PBS and cocktail of protease inhibitors (leupeptin, pepstatin, and aprotinin) prior to centrifugation at 15,000 × *g* for 15 min. The supernatant was stored at −80 °C for further analysis. The leftover portion of the right kidney was minced and homogenized in a cold lysis buffer containing Radio Immunoprecipitation Assay (RIPA) buffer, PMSF (Sigma), protease inhibitor cocktail (Roche), and PhosSTOP (Roche). Then, the homogenate was centrifuged at 15,000 × g for 15 min at 4 °C. Protein concentration was determined by the Bradford reagent (Bio-Rad, USA).

2.2.4. Relative kidney weight

Bodyweight of mice was recorded before sacrifice. The left kidney weight of mice was recorded during organ collection. The relative kidney weight was calculated using the following formula-(Almeer et al., 2019)

$$\text{Relativekidneyweight} = \frac{\textit{LeftKidneyweight}}{\textit{Bodyweigh}} \times 100$$

2.2.5. Determination of Pb concentration in blood and tissue samples

The Pb content of blood and tissue samples was determined following the protocol of the previously published article (Rana et al., 2020). Briefly, the samples were diluted with a mixture of 0.2% Triton-X 100, $(NH_4)_2HPO_4$, and water. A graphite furnace assembled with atomic absorption spectrometry (AAS) (Zeeman Atomic Absorption Spectrophotometer Z-5000, Hitachi, Japan) was used to determine the Pb concentration. The detection wavelength was set at 283.3 nm and the Pb concentration was calculated from the standard curve of pure Pb. The Pb content of blood and tissue samples was expressed as μg/dL and μg/g protein, respectively.

2.2.6. Determination of oxidative stress-related parameters

Oxidative stress is a common mechanism of cellular injury via lipid peroxidation. Thiobarbituric acid reactive substances (TBARS), a secondary byproduct of oxidative stress manifest as an indicator of LPO. For TBARS analysis, briefly, a 100 μL of sample and 20% of trichloroacetic acid (TCA) were mixed and centrifuged at 3000 rpm for 15 min. Then, the resultant supernatant was mixed with 15% thiobarbituric acid (TBA) following by the boiling for 30 min. After centrifugation at 3000 rpm for 15 min, the absorbance of supernatant was measured at 595 nm. The level of TBARS was calculated against a standard curve of Malondialdehyde (1, 1, 3, 3-tetraethoxypropane) (Rana et al., 2020).

The level of superoxide dismutase (SOD) and catalase (CAT) activity was assessed according to the protocol of Rana, Tangpong, and Rahman, 2020 (Rana et al., 2020). In case of SOD, 1 mL of Tris-EDTA buffer (pH 8.2) and pyrogallol solution (0.2 mM) were mixed. Thereafter, the sample (50 μL) was added to the mixture and absorbance was recorded at 420 nm for each 30 sec of 3 min duration using UV–vis spectrophotometer (JASC0 V- 630, Japan). The data were expressed as U/g of protein. For CAT activity, 2 mL of PBS was mixed with 10 μL of tissue homogenate. After that, 1 mL of 30 mM H_2O_2 solution was added to the mixture. The decomposition rate of H_2O_2 was recorded against PBS (blank) at 240 nm for each 30 sec of 3 min. The CAT activity was expressed as katal (k)/mg of protein.

2.2.7. Determination of kidney function parameters

To assess the kidney function, the blood urea nitrogen (BUN) and creatinine were determined using a bioassay system reagent kit (Hayward, CA, USA) in an automatic chemistry analyzer (KONE Lab20, Tokyo, JP). Besides, urine samples were collected for analyzing the creatinine and protein levels. Protein level was measured using UV–vis spectrophotometer (JASC0 V- 630, Japan).

2.2.8. Determination of inflammatory markers

2.2.8.1. Tumor necrosis factor-alpha (TNF-α) by ELISA. The level of plasma TNF-α was investigated using an enzyme-linked immunosorbent assay (ELISA) kit of R&D System, Minneapolis, MN, USA. The experiment was conducted following the supplied protocol by the manufacturer

2.2.8.2. Determination of TNF-α, COX-2, and iNOS expression by western blot. The protein expression was determined following the previously published report (Rana et al., 2020). In brief, a 40 μg of protein was loaded into each well of SDS polyacrylamide gel and run for electrophoresis (Bio-Rad Laboratories, Inc., California, USA) at 100 V. Afterward, the separated protein was transferred to a nitrocellulose membrane (Roche Diagnostics Corporation, Indianapolis, IN, USA) at 300 mA, 4 °C for 1.5 h. Then, the membrane was blocked with 5% skim milk in TBST (20 mM Tris–HCl, pH 7.4, 150 mM NaCl, 0.02% Tween 20). The membrane was then incubated overnight at 4 °C with primary antibody: TNF-α, COX-2, and iNOS (Cell Signaling Technology, Massachusetts, USA) followed by the washing with TBST 3X for 5 min. Following incubation with secondary antibody, the membrane was washed 3X for 5 min. After that, the intensity of protein band was determined by enhanced chemiluminescence detection kit (Bio-Rad, USA). The relative expression of protein was expressed as fold change compared to β-actin as control (Cell Signaling Technology, Massachusetts, USA).

2.2.9. Assessment of kidney histology and apoptosis

For analyzing kidney histology, tissue was fixed in 4% neutral-buffered formalin, dehydrated in a series of graded alcohol and then embedded in paraffin. The tissue was sectioned (4 μm) into a glass slide using Leica CM1950 Cryostat (Leica Microsystem,

Germany). The slides were hydrated and stained with hematoxylin and eosin (H & E) followed by air-drying. The photograph was investigated and captured using a light microscope (Olympus EX51, Olympus Corporation, Tokyo, Japan).

To investigate the extent of apoptosis, the frozen kidney tissue (-30 °C) was sectioned (7 μm) using a microtome (Leica Microsystem CM1950, Wetzlar, Germany) and fixed on glass slides using frozen mounting media (FSC 22 Mounting Media, Leica Biosystems, Harbourfront Center, Singapore). An *in situ* apoptosis detection kit (Abcam, Cambridge, UK) was used to evaluate the TUNEL positive cells in kidney section. The slides were investigated under a light microscope (Olympus EX51, Olympus Corporation, Tokyo, Japan), and the result was expressed as the number of TUNEL positive cells per 100 fields.

2.3. Statistical analysis

All data were expressed as mean ± standard error mean (SEM). Significant differences variables among groups were measured by one-way analysis of variance (ANOVA) followed by Newman–Keuls post hoc test using GraphPad Prism5 software. $P < 0.05$ was considered statistically significant.

3. Results

3.1. PASS prediction and molecular docking analysis

PASS analysis identified a total 15 phytoconstituents from TL leaves (See the supplementary **Table S1**). The result showed that individually these compounds were antitoxic/antidote, antioxidative stress element stimulant (HMOX1 expression enhancer; NF-E2-related factor 2 stimulants), calcium regulator, kidney function stimulant. Moreover, these phytoconstituents also possessed antioxidant and anti-inflammatory activity (See the supplementary **Table S2**).

Based on the PASS analysis and solubility in water, polyphenol compounds (e.g. caffeic acid, protocatechuic, and gallic acid) were selected for molecular docking which had better interaction with the assigned protein of interest (See the supplementary **Figure S1**). The docking values of phytoconstituents interaction with proteins were summarized in Table 4. For instance, protocatechuic acid which docked with IP_3R possesses the highest score −5.93 and the interacting residues are ARG 511, TYR 567, LYS569, ARG 269, ARG 265. Gallic acid with −5.9 docking score interacted with KEAP1 at ARG 483, SER 508. The order of compounds that showed the highest binding affinity to TNF-α, iNOS, COX-2, p38K, JNK, and NF-κB were protocatechuic acid (-5.66), protocatechuic (-6.258), gallic acid (-7.81), caffeic acid (-6.70), gallic acid (-6.62), and caffeic acid (-7.03), respectively.

The analyzed data of drug likeliness properties revealed that all of the phytochemicals that interacted with the assigned protein aforementioned earlier were resemble to be drug candidates (Table 5).

3.2. TL attenuated aberrant relative kidney weight

To validate the approach of treatment, the mice body weight, kidney weight, and body Pb content were investigated (Table 1). Study showed that no significant difference was observed between the mice body weight of Pb treated group and untreated control. In contrast, both kidney weight and % of relative kidney weight parameters were significantly different (1.38-fold) between untreated control and Pb treated group, while co-treatment of TL attenuated the parameters dose-dependently (1.04 and 0.92 for 100 and 200 mg/kgBW) (Table 1). On the other hand, the increment of blood and kidney Pb burden were closely associated with the elevated relative kidney weight in Pb treatment. Co-treatment with TL reduced the bodily Pb deposition in dose–response and significant manner except for blood Pb content (Table 1). The significant blood Pb content indicated that Pb deposition was crucial to elevate the % of relative kidney weight and uncovered as a probable pathological index in Pb-induced kidney toxicity.

3.3. TL mitigated the Pb-induced oxidative stress

To investigate the plausible mechanism of pathogenesis, the oxidative stress status was evaluated (Fig. 1). Treatment with Pb downregulated the activity of superoxide dismutase (SOD) and catalase (CAT) in kidney tissue as shown 1.36 and 3.36-fold, accordingly (Fig. 1**A-B**). Co-treatment of TL 200 mg/kgBW with PbAc significantly ($P < 0.05$) augmented the activity of SOD and CAT, however, vitamin E co-treatment failed to induce the SOD, and CAT in significant a passion. Furthermore, TL alone also enhanced CAT but not SOD activity (Fig. 1**A-B**). Besides, the plasma, RBC, and tissue TBARS levels were increased by 2.17, 2.0, and 1.32-fold, accordingly, when mice were treated with Pb (Fig. 1**C-E**). Coherent to the antioxidant activity, co-treatment of TL at both doses (100 and 200 mg/kgBW) remarkably ($P < 0.05$) suppressed the plasma, RBC, and tissue lipid peroxidation in response to oxidative stress (Fig. 1**C-E**). These findings dictated that TL co-treatment is effective in revising the reduced antioxidant enzymes (SOD and CAT activity) and increased lipid peroxidation.

3.4. TL modulated inflammation by suppressing the inflammatory mediators

To investigate the association of inflammation, plasma TNF-α level and tissue protein expression of TNF-α, COX-2, and iNOS were assessed (Fig. 2). The PbAc treated group exhibited ($P < 0.05$) almost 1.69-fold increased plasma TNF-α compared to untreated control group (Fig. 2**A**). Similarly, PbAc also upregulated the inflammatory tissue proteins expression such as TNF-α, COX-2, and iNOS were increased to 1.63, 3.17, and 1.57-fold, respectively

Table 1
Effect of TL extract on mice body weight, kidney weight, and Pb concentrations of PbAc treated mice.

Groups	Mice body weight	Kidney weight	% of relative kidney weight	Blood Pb (μg/dL)	Kidney Pb (μg/g protein)
Untreated Control	39.96 ± 0.80	0.34 ± 0.02	0.81 ± 0.03	1.83 ± 0.26	1.43 ± 0.08
PbAc (1% in DW)	39.96 ± 1.24	0.45 ± 0.02 [a]	1.12 ± 0.04 [a]	65.35 ± 0.83 [a]	52.70 ± 0.27 [a]
TL 200 mg/kgBW	44.39 ± 0.77[b]	0.40 ± 0.01[b]	0.90 ± 0.03[b]	1.69 ± 0.48[b]	1.37 ± 0.06[b]
Pb + TL 100 mg/kgBW	35.78 ± 1.68 [a,b]	0.37 ± 0.02[b]	1.04 ± 0.04 [a]	63.12 ± 1.59 [a]	45.45 ± 2.14 [a,b]
Pb + TL 200 mg/kgBW	39.20 ± 0.80	0.36 ± 0.01[b]	0.92 ± 0.04[b]	62.96 ± 1.25 [a]	42.50 ± 0.97 [a,b]
Pb + Vit-E 100 mg/kgBW	36.68 ± 1.04	0.37 ± 0.02[b]	1.01 ± 0.06 [a]	64.89 ± 2.45 [a]	52.90 ± 2.13 [a]
Vehicle Control	42.60 ± 0.80 [a]	0.33 ± 0.01[b]	0.77 ± 0.04[b]	1.89 ± 0.56 [a,b]	1.45 ± 0.09[b]

Data are presented as mean + SEM (n = 6). The multiple comparisons were analyzed by one-way analysis of variance followed by Newman–Keuls post hoc test. Here, [a] $P < 0.05$ vs untreated control, [b] $P < 0.05$ vs PbAc treated group.

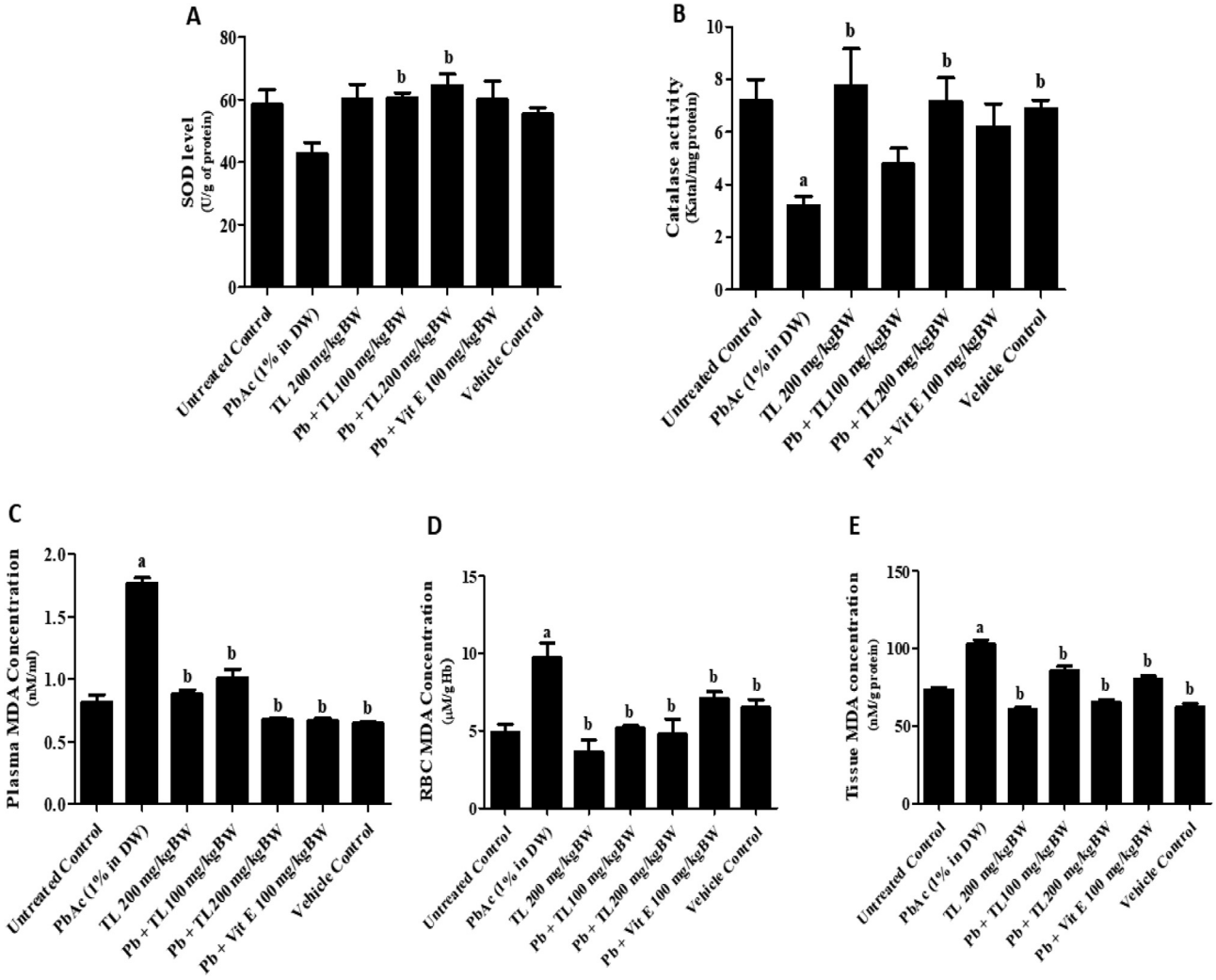

Fig. 1. Effect of TL extract on oxidative stress and antioxidant parameters of PbAc treated mice. Here, (A)- superoxide dismutase (SOD) level, (B)- catalase (CAT) activity, (C-E)- TBARS levels in the plasma, RBC, and kidney tissue, respectively. The values are presented as mean ± SEM (n = 6). The multiple comparisons were analyzed by one-way analysis of variance followed by Newman–Keuls post hoc test. Whereas, a $P < 0.05$ vs untreated control, b $P < 0.05$ vs PbAc treated group.

(Fig. 2**B-D**). As expected, co-treatment with TL at of 100, 200 mg/kgBW or vitamin E showed a significant deduction of circulating TNF-level compared to PbAc treated group ($P < 0.05$) (Fig. 2**A**). In addition, the expression of TNF-α, COX-2, and iNOS in the kidney were also downregulated in a dose-dependent manner when co-treated with TL or vitamin E (Fig. 2**B-D**). Thus, these findings illustrated that TL or vitamin E treatment can significantly attenuate the inflammation through suppressing the inflammatory mediators of PbAc induced kidney.

3.5. TL improved kidney function attenuating bodily biochemicals

To evaluate the renal function, the BUN and creatinine levels were evaluated in plasma sample, while the protein and creatinine levels, protein/creatinine ratio were estimated from urine sample (Table 2). Results showed that a significant ($P < 0.05$) increment of plasma BUN (1.37-fold) and creatinine (1.65-fold) levels were recorded in the mice treated with PbAc. Co-treatment of TL at both doses with PbAc declined the plasma BUN and creatinine levels significantly ($P < 0.05$), which were similar to that of vitamin E (1.93 and 1.4-fold, respectively).

Urine analysis study indicated that co-treatment of TL or vitamin E with PbAc significantly ($P < 0.05$) reduced the biochemical profile such as protein, creatinine levels, and protein/creatinine ratio than that of PbAc treated group (Table 2). These outcomes reflected the probability of TL's effects against Pb induced kidney dysfunction.

3.6. Renoprotective and anti-apoptotic effect of TL against Pb

To investigate the magnitude of kidney damage, kidney tissues were stained with H&E and TUNEL assay (Figs. 3 and 4). The figure of control group represents the normal structure of glomerulus, proximal and distal in comparison to PbAc treated kidney, which shows the profound (+ + +) glomerular swelling, degenerative tubules, and interstitial inflammation (Fig. 3 **and** Table 3). These architectural changes of kidney tissue were returned to normal when co-treated with TL or vitamin E as shown by the grading score 0 (Fig. 3 **and** Table 3**)**.

Successively, findings of the TUNEL assay also corroborated the outcome of H&E staining. Likewise, the degeneration of nephron architecture, an outnumber (5.75-fold) of cell death were reported in PbAC treated group compared to untreated control ($P < 0.05$) (Fig. 4). Co-treatment of TL at different doses declined the dead cell number dose-dependently. Interestingly, the outcome was promising for TL 200 mg/kgBW (2.97-fold vs PbAc), which was better than

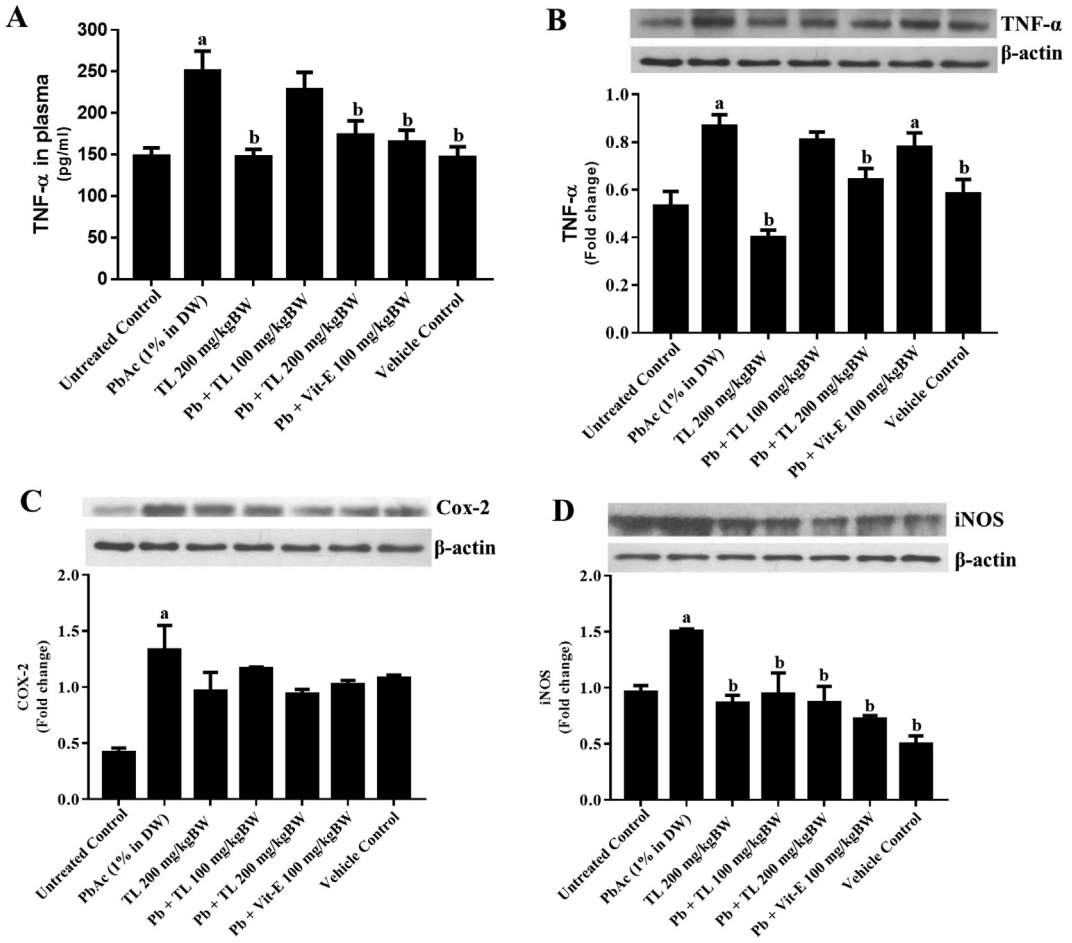

Fig. 2. Effect of TL extract on inflammatory parameters of PbAc treated mice. Here, (A)- TNF-α level in plasma by ELISA assay, (B-D)- protein expression and quantification of TNF-α, COX-2, and iNOS in the kidney, respectively. The values are presented as mean ± SEM (n = 6). The multiple comparisons were analyzed by one-way analysis of variance followed by Newman–Keuls post hoc test. Whereas, a $P < 0.05$ vs untreated control, b $P < 0.05$ vs PbAc treated group.

Table 2
Effect of TL extract on kidney function in PbAc treated mice.

	Plasma		Urine		
Groups	BUN (mg/dL)	Creatinine (mg/dL)	Protein (mg/dL)	Creatinine (mg/dL)	Protein/Creatinineration
Untreated Control	32.80 ± 1.01	0.23 ± 0.03	20.80 ± 0.02	15.20 ± 1.17	1.36
PbAc (1% in DW)	45.04 ± 4.49 [a]	0.38 ± 0.05 [a]	27.60 ± 0.05 [a]	9.60 ± 1.62 [a]	2.88 [a]
TL 200 mg/kgBW	29.40 ± 1.59	0.22 ± 0.03	17.90 ± 0.02 [a,b]	15.50 ± 2.08[b]	1.15[b]
Pb + TL 100 mg/kgBW	20.33 + 0.41[b]	0.33 + 0.05[b]	24.10 ± 0.02 [a,b]	11.07 ± 0.14	2.18 [a,b]
Pb + TL 200 mg/kgBW	23.00 + 0.71[b]	0.36 + 0.03[b]	22.20 ± 0.05 [a,b]	18.80 ± 3.04[b]	1.18[b]
Pb + Vit E 100 mg/kgBW	23.33 + 1.02[b]	0.27 + 0.04[b]	19.50 ± 0.04[b]	22.10 ± 0.96[b]	1.13[b]
Vehicle Control	19.00 ± 0.41	0.26 ± 0.02	21.30 ± 0.02[b]	19.80 ± 1.68[b]	1.08[b]

Data are presented as mean + SEM (n = 6). The multiple comparisons were analyzed by one-way analysis of variance followed by Newman–Keuls post hoc test. Here, [a] $P < 0.05$ vs untreated control, [b] $P < 0.05$ vs PbAc treated group.

vitamin E (1.79-fold vs PbAc). In addition, there was no toxic effect was observed by TL 200 mg/kgBW or vitamin E vehicle, respectively (Fig. 4). Thus, TL has the ability to restore the architectural alterations of kidney by Pb.

4. Discussion

This study exerted the ability of PbAc to induce kidney toxicity by initiating the oxidative stress, inflammation, and cell death, which is resulted in kidney dysfunction and aberrant architecture of nephron. TL was effective in reversing all alterations that caused by PbAc. The possible underpinning protective mechanism could be due to its capability to activate Nrf-2, decrease cytosolic Ca^{2+}, downregulate the inflammatory mediators and pathways (MAPK and NF-κB).

Lead intoxication is a global concern and is closely associated with industrialization. Therefore, its remedies such as chelating therapy are requisite based on the magnitude of toxicity (Rana et al., 2020) Persistent usage of antidote alone ($CaNa_2EDTA$, Dimercaprol, Dimercaprol) or in combination ($CaNa_2EDTA$ with Dimercaprol) can develop adverse effects such as encephalopathy,

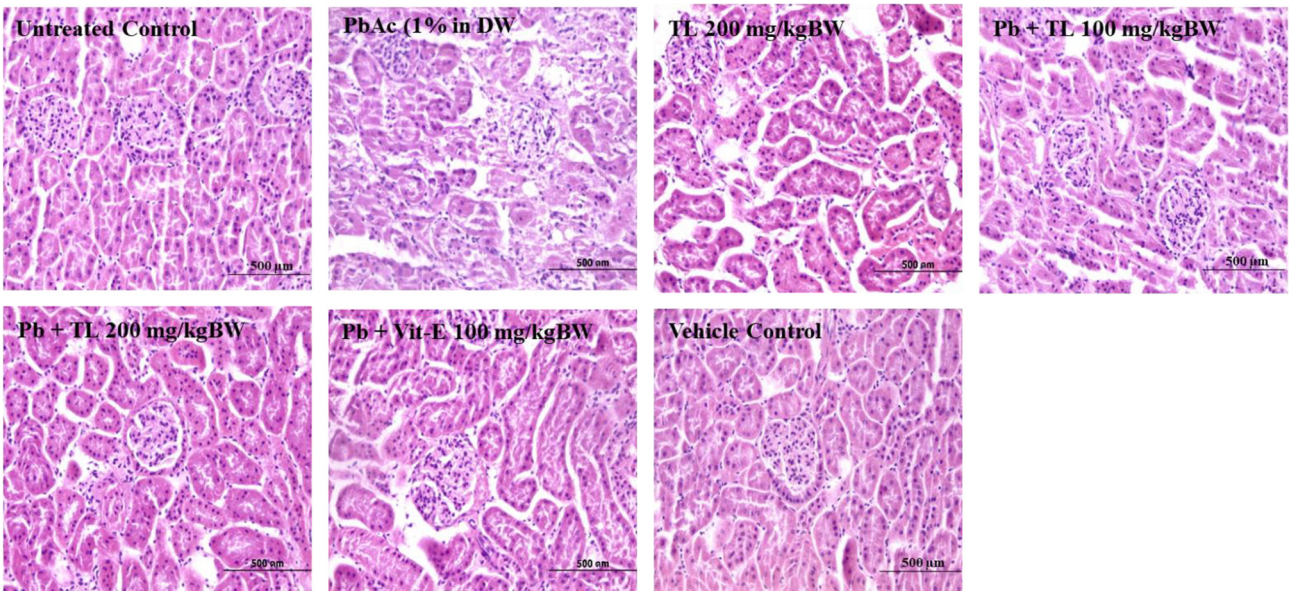

Fig. 3. Histopathological alterations in the kidney of experimental mice. Kidney tissues were stained with hematoxylin and eosin staining. Histological alteration of kidney was mainly observed in the cortex region, both in proximal (PT) and distal tubules (DT). Untreated Control, TL 200 mg/kgBW, and Vehicle Control groups showed normal renal architectures. In contrast, only PbAc exposed group (PbAc 1% in DW) showed the presence of tubular necrosis such as cloudy swelling of PT, shrinkage of both DT and PT. However, co-treatment with TL (100 and 200 mg/kgBW) and vitamin E (100 mg/kgBW) significantly restored the renal alterations compared to only PbAc exposed group (PbAc 1% in DW).

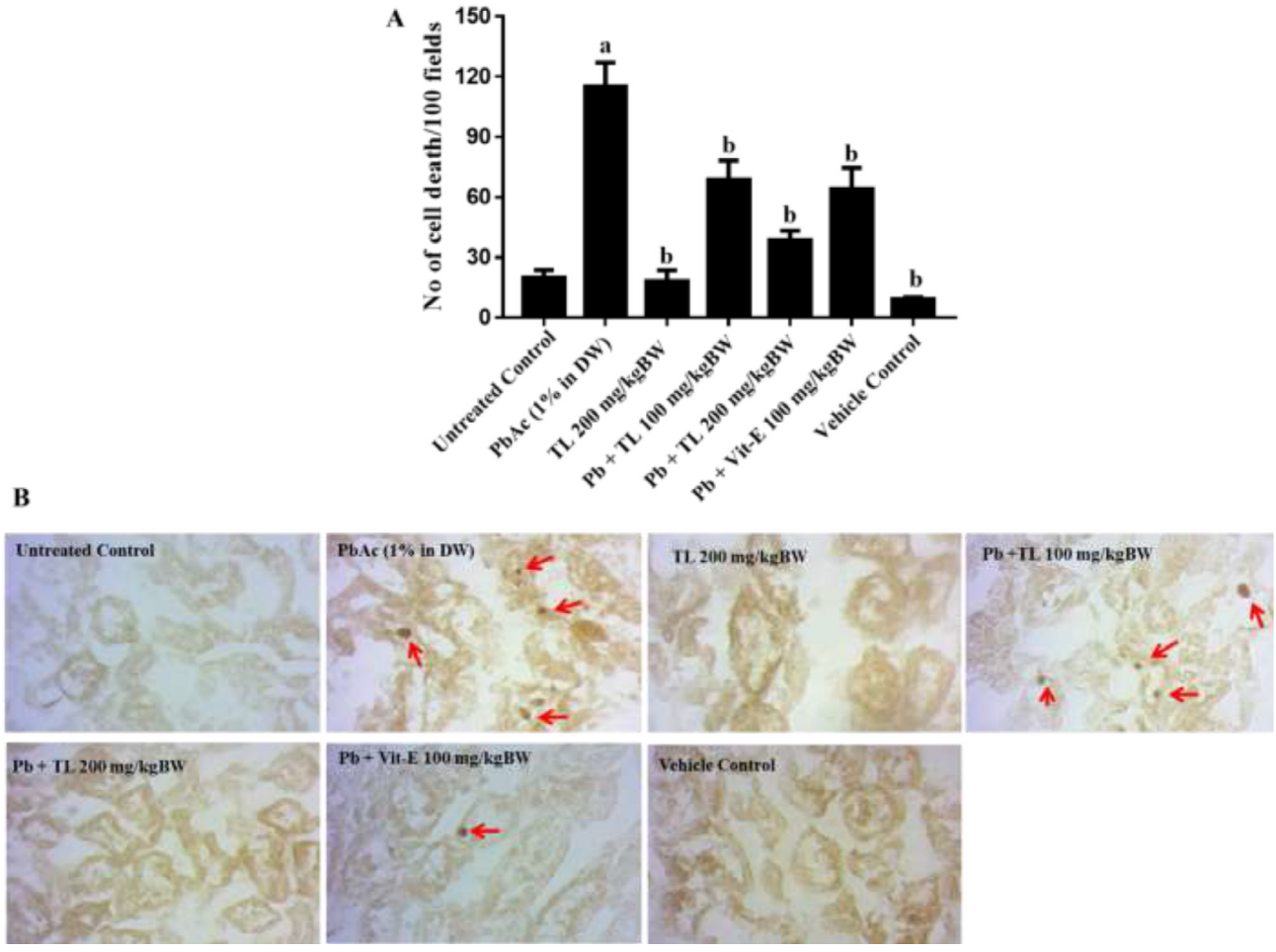

Fig. 4. Evaluation of the kidney apoptosis of PbAc treated mice kidney by terminal deoxynucleotidyl transferase dUTP nick end labeling (TUNEL) assay. (A)-Quantification of TUNEL positive cells in the kidney tissue section. The values are presented as mean ± SEM (n = 6). The multiple comparisons were analyzed by one-way analysis of variance followed by Newman–Keuls post hoc test. Whereas, a $P \leq 0.05$ vs untreated control, b $P \leq 0.05$ vs PbAc treated group. (B)- TUNEL positive cells were indicated by the red arrow in kidney tissue section (original magnification x400).

Table 3
Effect of TL extract on kidney damage parameters in PbAc treated mice.

Groups	Hydropic degeneration changes in tubules	Glomerular damage	Inflammatory cellular infiltration
Untreated Control	0	0	0
PbAc (1% in DW)	+ + +	+ + +	+ + +
TL 200 mg/kgBW	0	0	0
Pb + TL 100 mg/kgBW	+ +	+ +	+ +
Pb + TL 200 mg/kgBW	0	0	0
Pb + Vit-E 100 mg/kgBW	0	0	0
Vehicle Control	0	0	0

Histological evaluations of kidney tissues (n = 6). Here, +++ represents profound damage or diffuse damage to more than 50% of the tissue, ++ indicates moderate damage or damage scattered between 10 and 50% of tissue, + is considered as mild damage or random in<10% of the tissue, and 0 = no damage.

kidney damage, cardiac disorder (tachycardia), hepatic enzyme upregulation, hematological disorder, essential metal ion (Zn) depletion, and vomiting (Schroder et al., 2015). Therefore, researchers are looking for alternative sources of therapeutics like herbal medicine to mitigate the clinical conditions based on their ethnobotanical study, which was also the aim of our study. The research on PbAc toxicity has been under investigation since the long, but the toxicodynamics of Pb on the kidney is yet to be developed. In general, oxidative stress is termed as the commonly employed mechanism in Pb-induced nephrotoxicity; an outcome of excessive ROS (Kelainy et al., 2019) exclusively superoxide anion (Gargouri et al., 2013) production. In this context, we postulated that attenuation of oxidative stress and its downstream player by TL could be the plausible protective role against PbAc induced kidney toxicity. Our current study demonstrated that co-administration of TL with PbAc reduced the oxidative stress with enhanced SOD and CAT activity as well as reduced Pb accumulation, which were in agreement with a previous study (Hasanein and Riahi, 2018). Hence, PASS analysis of TL phytoconstituents (Supplementary file 1) and the previous study from our lab revealed that TL is a potent antioxidant and could possess the chelating effect as a form of antioxidant activity (Rana and Tangpong, 2017). The phenolic compound present in the TL leaves exclusively caffeic acid, gallic acid and protocatechuic acid are previously reported to protect kidney against oxidative stress enhancing the endogenous antioxidant (Kohansal et al., 2019; Rehman and Sultana, 2011; Yamabe et al., 2015). However, there is an ambiguity to explain the failure of TL to reduce blood Pb deposition.

Shreds of evidence suggested that Pb intoxication alters the histological integrity of the kidney as well as kidney functions. According to our current study, TL restored the PbAc induced all histological alterations such as hydropic degeneration changes in tubules, glomerular damage and inflammatory cellular infiltration. These results were in agreement with the previous studies (Mao et al., 2016; Zhang et al., 2019). Consistently, tissue apoptosis analysis strongly corroborates with the histopathological findings and kidney dysfunctions. For example, higher number of cell death (TUNEL positive) was evidenced in PbAc treated mice, while TL effectively protected the cell from death. This result could be due to the counteracting effect of TL against ROS mediated activation of caspase-3 and caspase-9 (He et al., 2016; Moneim et al., 2016; Siddarth et al., 2018), exclusively by protocatechuic acid, caffeic acid and gallic acid (Mard et al., 2015; Trumbeckaite et al., 2017; Yamabe et al., 2015). To activate caspase cascades, DNA fragmentation is a prerequisite (McIlwain et al., 2013), which was actively achieved by PbAc in the kidney (Kelainy et al., 2019). Our previous report uncovered that TL can protect DNA from PbAc induced toxicity (Rana and Tangpong, 2017). However, the current study did not exclude any other means of programmed cell death, e.g pyroptosis.

The interplay between inflammation, ROS, and Pb toxicity is well documented (Wang et al., 2016). Pb mediated ROS abundance can function as signaling messengers to NF-κB (Gloire et al., 2006). Activated NF-κB is then translocated to the nucleus, where it regulates the transcription of inflammatory genes such as TNF-α, COX-2, and iNOS ((Bhaskar et al., 2011; Gloire et al., 2006; Nair et al., 2006), which is coherent with our current findings. Moreover, ERK/JNK/p38 pathway is also involved in Pb-induced ROS mediated inflammation and tubular damage (Wang et al., 2016). According to Meissner, Viehmann, and Kurts, 2019, Danger-associated–molecular pattern molecules (DAMPs) generated from damaged kidney could also induce the inflammation (Meissner et al., 2019). In our current study, TL attenuated kidney inflammation through the downregulation of inflammatory mediators possibly by interfering with NF-κB, MAPK pathway. Accumulated study reported that caffeic acid, gallic acid and protocatechuic acid are able to limit the inflammation by reducing cytokines like IL-1β, TNF-α, monocyte chemoattractant protein 1 (MCP-1) and myeloperoxidase (MPO) activity (Chao et al., 2010; Owumi et al., 2020; Semaming et al., 2015).

According to previous studies, TL leaf also contains water soluble phenolic compounds along with other water insoluble constituents (Chan et al., 2011; Oonsivilai et al., 2008; Ratchadaporn, 2006). To explore the possible pathway of the protective effect of TL, PASS analysis of the available phytoconstituents of TL was employed. Based on PASS analysis and our recent review, we assumed that the activity of TL phytoconstituents against PbAc, might be due to the capability to induce Nrf-2 and to limit Ca^{2+} ion in the cytosol (activation of IP_3R), or to modulate the MAPK, NF-kB pathways. In the meantime, Trumbeckaite and colleagues reported that ester of caffeic acid and phenethyl alcohol is capable to induce mitochondrial calcium uptake and protects kidney cells from ischemia-induced necrosis (Trumbeckaite et al., 2017). Besides, protocatechuic acid, caffeic acid and gallic acid also possess the activity to inhibit the activation of NF-kB and MAPK pathways (Ahad et al., 2015; Huang et al., 2018; Ma et al., 2018; Takakura et al., 2018). In agreement with our previous study, the current docking study suggested that among phytochemicals polyphenols were the most active constituents to interact with a high affinity toward IP_3R, Keap-1, JNK, p38, iNOS, TNF-α, COX-2, which support our hypothesis (Rana et al., 2020). Concomitant to current findings, previous studies also demonstrated that phenolic content is highly effective against Pb induced toxicity via intervening NF-kB and MAPK activation (Gargouri et al., 2013; Wang et al., 2016).

In a nutshell, the above findings suggested that PbAc caused kidney damage and impaired function through oxidative stress, inflammation, and apoptosis. TL ameliorated all the aberrant indices via inducing Nrf-2 and suppressing IP_3R, MAPK, NF-kB pathways. Therefore, TL might be applicable to treat Lead-mediated kidney complications, though extensive studies and clinical trials are needed.

Table 4
Phyto-constituents of TL extract attenuates oxidative stress and inflammation via interacting with IP3R, KEAP-1, TNF-α, iNOS, COX-2, p38 kinase, JNK, and NF-kB.

Compound names	IP_3R (PDB:3UJ0)			KEAP-1 (PDB:5CGJ)			TNF-α (PDB: 2AZ5)			iNOS (PDB: 3E67)			**COX-2 (PDB: 5KIR)**		
	Docking score	Glide energy	Interacting Residues	Docking score	Glide energy	Interacting Residues	Docking score	Glide energy	Interacting Residues	Docking score	Glide energy	Interacting Residues	Docking score	Glide energy	Interacting Residues
Caffeic acid	−4.16	−22.10	ARG 269 ARG 511 ARG 504 LYS 569	−5.05	−25.40	SER 555 GLN 530	−5.52	−26.02	LEU B:120 TYR B:119 SER B:160	−4.977	−26.18	GLU 371	−6.26	−25.58	SER 530 ARG 120
Protocatechuic acid	−5.93	−27.62	ARG 511 TYR 567 LYS569 ARG 269 ARG 265	−5.75	−21.68	ARG 483 SER 508	−5.66	−21.20	TYR B:151 SER B: 60	−6.258	−25.08	TRP 366 SER 436	−7.26	−27.65	NONE
Gallic acid	−5.68	−26.42	ARG 265 ARG 269 ARG 511 TYR 567 LYS 569	−5.9	−23.72	ARG 483 SER 508	−5.57	−22.47	TYR B:119 SER B:60	−4.97	−22.73	GLU 371	−7.81	−32.34	MET 522

Compound names	P38 KINSAE (PDB: 2YIS)			JNK (PDB: 3OY1)			NFκB (PDB: 4KIK)		
	Docking score	Glide energy	Interacting Residues	Docking score	Glide energy	Interacting Residues	Docking score	Glide energy	Interacting Residues
Caffeic acid	−6.70	−28.78	ALA 111 GLY 110 MET 109 HID 107 LYS 53	−5.91	−29.33	MET 149 LYS 93	−7.03	−30.33	CYS 99 GLU 97 ASP 166 LYS 44
Protocatechuic acid	−6.41	−25.62	GLY 110 MET 109 HID 107	−5.87	−24.20	LEU 144 LYS 93	−6.10	−24.03	ASP 103 CYS 99
Gallic acid	−6.47	−26.78	GLY 110 MET 109 HID 107	−6.62	−29.66	ILE 70 MET 149	−5.99	−24.78	ASP 103 CYS 99

Table 5
Drug likeliness properties of TL extract.

Compound name	PubChem CID	Drug-likeliness properties			
		MW (g/mol)	HB donor	HB acceptor	QPlogPo/w
Caffeic acid	689,043	180.16	3	3.5	0.557
Protocatehuic acid	72	154.122	3	3.5	0.032
Gallic acid	370	170.121	4	4.25	−0.568

QikProp module of Maestro 11 (Schrodinger) was used to project the drug-likeliness properties of these seven compounds. Here, M.W represents Molecular weight; HB donor represents donation of hydrogen bond by solute; HB acceptor, number of hydrogen bonds received by the solute; QPlogPo/w, Predicted octanol/water partition coefficient. Compounds that meet at least three properties such as MW- < 500, HB donor- ≤5, HB acceptor- ≤10, QPlogPo/w- (−) 2.0–6.5, were considered to possess drug-like properties.

Ethical Approval

Approval for the use of animals was given by the Animal Care and Use Committee (ACUC) of Walailak University, Thailand. Animals were handled as stipulated by the guidelines for the use of animals set by the ACUC of the university, with the Animal Ethics Approval Certificate number: 002/2013.

Funding

This whole study was financially supported by graduate research fund, Walailak University, Thailand (Grant no. WU59122).

CRediT authorship contribution statement

Mohammad Nasiruddin Rana: Conceptualization, Formal analysis, Writing - original draft, Writing - review & editing. **Naymul Karim:** Formal analysis, Writing - original draft, Writing - review & editing. **Suksan Changlek:** Writing - review & editing. **Md. Atiar Rahman:** Writing - review & editing. **Jitbanjong Tangpong:** Supervision, Resources, Validation, Writing - review & editing. **Dina Hajjar:** . **Walla Alelwani:** . **Arwa A. Makki:** .

Declaration of Competing Interest

The authors declare that they have no known competing financial interests or personal relationships that could have appeared to influence the work reported in this paper.

Acknowledgement

Mohammed Sohel Chowdhury, Department of Pharmacy, International Islamic University Chittagong, Bangladesh, for his technical assistance regarding Schrodinger Software. This reseach was partilly supported by the new strategic research (P2P) project, Walailak University, Thailand.

Appendix A. Supplementary data

Supplementary data to this article can be found online at https://doi.org/10.1016/j.sjbs.2020.08.016.

References

Ademuyiwa, O., Ugbaja, R.N., Rotimi, S.O., Abam, E., Okediran, B.S., Dosumu, O.A., Onunkwor, B.O., 2007. Erythrocyte acetylcholinesterase activity as a surrogate indicator of lead-induced neurotoxicity in occupational lead exposure in Abeokuta. Nigeria. Environ. Toxicol. Pharmacol. 24, 183–188. https://doi.org/10.1016/j.etap.2007.05.002.

Ahad, A., Ahsan, H., Mujeeb, M., Siddiqui, W.A., 2015. Gallic acid ameliorates renal functions by inhibiting the activation of p38 MAPK in experimentally induced type 2 diabetic rats and cultured rat proximal tubular epithelial cells. Chem. Biol. Interact. 240, 292–303. https://doi.org/10.1016/j.cbi.2015.08.026.

Almeer, R.S., Albasher, G., Alotibi, F., Alarifi, S., Ali, D., Alkahtani, S., 2019. *Ziziphus spina-christi* Leaf Extract Suppressed Mercury Chloride-Induced Nephrotoxicity via Nrf2-Antioxidant Pathway Activation and Inhibition of Inflammatory and Apoptotic Signaling. Oxid. Med. Cell. Longev. 2019, 5634685. https://doi.org/10.1155/2019/5634685.

Azeh Engwa, G., Udoka Ferdinand, P., Nweke Nwalo, F., N. Unachukwu, M., 2019. Mechanism and Health Effects of Heavy Metal Toxicity in Humans, in: Poisoning in the Modern World - New Tricks for an Old Dog? IntechOpen. https://doi.org/10.5772/intechopen.82511

Bhaskar, S., Shalini, V., Helen, A., 2011. Quercetin regulates oxidized LDL induced inflammatory changes in human PBMCs by modulating the TLR-NF-κB signaling pathway. Immunobiology 216, 367–373. https://doi.org/10.1016/j.imbio.2010.07.011.

Centers for Disease control and Prevention, 2020. Sources of Lead | Lead | CDC [WWW Document] accessed 8.2.20 https://www.cdc.gov/nceh/lead/prevention/sources.htm, .

Chan, E.W.C., Eng, S.Y., Tan, Y.P., Wong, Z.C., 2011. Phytochemistry and Pharmacological Properties of Thunbergia laurifolia: A Review. Pharmacogn. J. 3, 1–6. https://doi.org/10.5530/pj.2011.24.1.

Chao, C.Y., Mong, M.C., Chan, K.C., Yin, M.C., 2010. Anti-glycative and anti-inflammatory effects of caffeic acid and ellagic acid in kidney of diabetic mice. Mol. Nutr. Food Res. 54, 388–395. https://doi.org/10.1002/mnfr.200900087.

Filimonov, D.A., Lagunin, A.A., Gloriozova, T.A., Rudik, A.V., Druzhilovskii, D.S., Pogodin, P.V., Poroikov, V.V., 2014. Prediction of the Biological Activity Spectra of Organic Compounds Using the Pass Online Web Resource. Chem. Heterocycl. Compd. 50, 444–457. https://doi.org/10.1007/s10593-014-1496-1.

Gargouri, M., Magné, C., Dauvergne, X., Ksouri, R., El Feki, A., Metges, M.-A.G., Talarmin, H., 2013. Cytoprotective and antioxidant effects of the edible halophyte Sarcocornia perennis L. (swampfire) against lead-induced toxicity in renal cells. Ecotoxicol. Environ. Saf. 95, 44–51. https://doi.org/10.1016/j.ecoenv.2013.05.011.

Gloire, G., Legrand-Poels, S., Piette, J., 2006. NF-kappaB activation by reactive oxygen species: fifteen years later. Biochem. Pharmacol. 72, 1493–1505. https://doi.org/10.1016/j.bcp.2006.04.011.

Hasanein, P., Riahi, H., 2018. Preventive use of berberine in inhibition of lead-induced renal injury in rats. Environ. Sci. Pollut. Res. 25, 4896–4903. https://doi.org/10.1007/s11356-017-0702-y.

He, X.Y., Yuan, L.Y., Li, Y.T., Li, M., Chen, Y., Yuan, H., Wu, J., Guo, C.Z., Li, J., 2016. Cytotoxic Responses and Apoptosis in Rat Kidney Epithelial Cells Exposed to Lead. Biomed. Environ. Sci. 29, 529–533. https://doi.org/10.3967/bes2016.070.

Huang, X., Xi, Y., Pan, Q., Mao, Z., Zhang, R., Ma, X., You, H., 2018. Caffeic acid protects against IL-1β-induced inflammatory responses and cartilage degradation in articular chondrocytes. Biomed. Pharmacother. 107, 433–439. https://doi.org/10.1016/j.biopha.2018.07.161.

Junsi, M., Siripongvutikorn, S., 2016. Thunbergia laurifolia, a traditional herbal tea of Thailand: Botanical, chemical composition, biological properties and processing influence. Int. Food Res. J. 23, 923–927.

Kanchanapoom, T., Kasai, R., Yamasaki, K., 2002. Iridoid glucosides from Thunbergia laurifolia. Phytochemistry 60, 769–771.

Kelainy, E.G., Ibrahim Laila, I.M., Ibrahim, S.R., 2019. The effect of ferulic acid against lead-induced oxidative stress and DNA damage in kidney and testes of rats. Environ. Sci. Pollut. Res. 26, 31675–31684. https://doi.org/10.1007/s11356-019-06099-6.

Kohansal, P., Rajai, N., Dehpour, A.R., Rashidian, A., Shafaroodi, H., 2019. The protective effect of acute pantoprazole pretreatment on renal ischemia/reperfusion injury in rats. Fundam. Clin. Pharmacol. 33, 405–411. https://doi.org/10.1111/fcp.12451.

Lowry, J.A., 2010. Oral chelation therapy for patients with lead poisoning. Am. Acad. Pediatr. 116, 1036–1046.

Ma, Y., Chen, F., Yang, S., Chen, B., Shi, J., 2018. Protocatechuic acid ameliorates high glucose-induced extracellular matrix accumulation in diabetic nephropathy. Biomed. Pharmacother. 98, 18–22. https://doi.org/10.1016/j.biopha.2017.12.032.

Mao, L., Qian, Q., Li, Q., Wei, S., Cao, Y., Hao, Y., Liu, N., Wang, Q., Bai, Y., Zheng, G., 2016. Lead selenide nanoparticles-induced oxidative damage of kidney in rats. Environ. Toxicol. Pharmacol. 45, 63–67. https://doi.org/10.1016/j.etap.2016.05.015.

Mard, S.A., Mojadami, S., Farbood, Y., Gharib Naseri, M.K., 2015. The anti-inflammatory and anti-apoptotic effects of gallic acid against mucosal inflammation- and erosions-induced by gastric ischemia-reperfusion in rats. Vet. Res. forum an Int. Q. J. 6, 305–311.

McIlwain, D.R., Berger, T., Mak, T.W., 2013. Caspase functions in cell death and disease. Cold Spring Harb. Perspect. Biol. 5. https://doi.org/10.1101/cshperspect.a008656. a008656 a8656.

Meissner, M., Viehmann, S.F., Kurts, C., 2019. DAMPening sterile inflammation of the kidney. Kidney Int. 95, 489–491. https://doi.org/10.1016/j.kint.2018.12.007.

Moneim, A., Dkhil, M., Al-Khalifa, M., Al-Quraishy, S., Zrieq, R., 2016. Indigofera oblongifolia mitigates lead-acetate-induced kidney damage and apoptosis in a rat model. Drug Des. Devel. Ther. 10, 1847. https://doi.org/10.2147/DDDT.S105511.

Nair, M.P., Mahajan, S., Reynolds, J.L., Aalinkeel, R., Nair, H., Schwartz, S.A., Kandaswami, C., 2006. The flavonoid quercetin inhibits proinflammatory cytokine (tumor necrosis factor alpha) gene expression in normal peripheral blood mononuclear cells via modulation of the NF-kappa beta system. Clin. Vaccine Immunol. 13, 319–328. https://doi.org/10.1128/CVI.13.3.319-328.2006.

Oonsivilai, R., Mario, G.F., Ningsanond, S., 2008. Antioxidant activity and Cytotoxicity of Rang Chuet (Thunbergia laurifolia Lindl.) Extracts. Asian J. Food Agro-Industry 1, 116–128.

Orr, S.E., Bridges, C.C., 2017. Chronic Kidney Disease and Exposure to Nephrotoxic Metals. Int. J. Mol. Sci. 18, 1039. https://doi.org/10.3390/ijms18051039.

Owumi, S., Najophe, E.S., Farombi, E.O., Oyelere, A.K., 2020. Gallic acid protects against Aflatoxin B1-induced oxidative and inflammatory stress damage in rats kidneys and liver. J. Food Biochem. 1, 1–12. https://doi.org/10.1111/jfbc.13316.

Tejasen, P., Thongthapp, C., 1980. The study of the insecticide antitoxicity of Thunbergia laurifolia Linn. Chiang Mai Med. J. 19, 105–114.

Patrick, L., 2006. Lead toxicity part II: the role of free radical damage and the use of antioxidants in the pathology and treatment of lead toxicity. Altern. Med. Rev. 11, 114–127.

Phyu, M.P., Tangpong, J., 2013. Protective effect of Thunbergia laurifolia (Linn.) on lead induced acetylcholinesterase dysfunction and cognitive impairment in mice. Biomed Res. Int. 2013, 186098. https://doi.org/10.1155/2013/186098

Rana, M.N., Tangpong, J., 2017. In Vitro Free Radical Scavenging and Anti-Genotoxic Activities of Thunbergia Laurifolia Aqueous Leaf Extract. J. Heal. Res. 31, 127–133.

Rana, M.N., Tangpong, J., Rahman, M.A., 2020. Xanthones protects lead-induced chronic kidney disease (CKD) via activating Nrf-2 and modulating NF-kB. MAPK pathway. Biochem. Biophys. Reports 21, 100718. https://doi.org/10.1016/j.bbrep.2019.100718.

Rana, M.N., Tangpong, J., Rahman, M.M., 2018. Toxicodynamics of Lead, Cadmium, Mercury and Arsenic- induced kidney toxicity and treatment strategy: A mini review. Toxicol. Reports 5, 704–713. https://doi.org/10.1016/j.toxrep.2018.05.012.

Ratchadaporn, O., 2006. Functional and nutraceutical properties of Rang Chuet (Thunbergia laurifolai lindl.) extracts. Suranaree University of Technology.

Rehman, M.U., Sultana, S., 2011. Attenuation of oxidative stress, inflammation and early markers of tumor promotion by caffeic acid in Fe-NTA exposed kidneys of Wistar rats. Mol. Cell. Biochem. 357, 115–124. https://doi.org/10.1007/s11010-011-0881-7.

Rocejanasaroj, A., Tencomnao, T., Sangkitikomol, W., 2014. Thunbergia laurifolia extract minimizes the adverse effects of toxicants by regulating P-glycoprotein activity, CYP450, and lipid metabolism gene expression in HepG2 cells. Genet. Mol. Res. 13, 205–219. https://doi.org/10.4238/2014.January.10.12.

Schroder, A.P., Tilleman, J.A., II, E.M.D., 2015. Lead toxicity and chelation therapy. US Pharm. 40.

Semaming, Y., Pannengpetch, P., Chattipakorn, S.C., Chattipakorn, N., 2015. Pharmacological properties of protocatechuic Acid and its potential roles as complementary medicine. Evid. Based. Complement. Alternat. Med. 2015, 593902. https://doi.org/10.1155/2015/593902.

Siddarth, M., Chawla, D., Raizada, A., Wadhwa, N., Banerjee, B.D., Sikka, M., 2018. Lead-induced DNA damage and cell apoptosis in human renal proximal tubular epithelial cell: Attenuation via N-acetyl cysteine and tannic acid. J. Biochem. Mol. Toxicol. 32, e22038. https://doi.org/10.1002/jbt.22038.

Takakura, K., Takatou, S., Tomiyama, R., Le, T.M., Nguyen, D.T., Nakamura, Y., Konishi, T., Matsugo, S., Hori, O., 2018. Inhibition of nuclear factor-κB p65 phosphorylation by 3,4-dihydroxybenzalacetone and caffeic acid phenethyl ester. J. Pharmacol. Sci. 137, 248–255. https://doi.org/10.1016/j.jphs.2018.07.003.

Tangpong, J., Satarug, S., 2010. Alleviation of lead poisoning in the brain with aqueous leaf extract of the Thunbergia laurifolia (Linn.). Toxicol. Lett. 198, 83–88. https://doi.org/10.1016/j.toxlet.2010.04.031.

Trumbeckaite, S., Pauziene, N., Trumbeckas, D., Jievaltas, M., Baniene, R., 2017. Caffeic Acid Phenethyl Ester Reduces Ischemia-Induced Kidney Mitochondrial Injury in Rats. Oxid. Med. Cell. Longev. 2017, 1697018. https://doi.org/10.1155/2017/1697018.

Vega-Dienstmaier, J.M., Salinas-Piélago, J.E., Gutiérrez-Campos, M. del R., Mandamiento-Ayquipa, R.D., Yara-Hokama, M. del C., Ponce-Canchihuamán, J., Castro-Morales, J., 2006. Lead levels and cognitive abilities in Peruvian children. Rev. Bras. Psiquiatr. 28, 33–9. https://doi.org//S1516-44462006000100008

Wang, H., Li, D., Hu, Z., Zhao, S., Zheng, Z., Li, W., 2016. Protective Effects of Green Tea Polyphenol Against Renal Injury Through ROS-Mediated JNK-MAPK Pathway in Lead Exposed Rats. Mol. Cells 39, 508–513 https://doi.org/10.14348/molcells.2016.2170.

Wang, H., Wang, Z.-K., Jiao, P., Zhou, X.-P., Yang, D.-B., Wang, Z.-Y., Wang, L., 2015. Redistribution of subcellular calcium and its effect on apoptosis in primary cultures of rat proximal tubular cells exposed to lead. Toxicology 333, 137–146. https://doi.org/10.1016/j.tox.2015.04.015.

Wonkchalee, O., Boonmars, T., Aromdee, C., Laummaunwai, P., Khunkitti, W., Vaeteewoottacharn, K., Sriraj, P., Aukkanimart, R., Loilome, W., Chamgramol, Y., Pairojkul, C., Wu, Z., Juasook, A., Sudsarn, P., 2012. Anti-inflammatory, antioxidant and hepatoprotective effects of Thunbergia laurifolia Linn. on experimental opisthorchiasis. Parasitol. Res. 111, 353–359. https://doi.org/10.1007/s00436-012-2846-5.

Wright, W.C., Chenge, J., Wang, J., Girvan, H.M., Yang, L., Chai, S.C., Huber, A.D., Wu, J., Oladimeji, P.O., Munro, A.W., Chen, T., 2020. Clobetasol Propionate Is a Heme-Mediated Selective Inhibitor of Human Cytochrome P450 3A5. J. Med. Chem. https://doi.org/10.1021/acs.jmedchem.9b02067.

Yamabe, N., Park, J.Y., Lee, Seungyong, Cho, E.J., Lee, Sanghyun, Kang, K.S., Hwang, G.S., Kim, S.N., Kim, H.Y., Shibamoto, T., 2015. Protective effects of protocatechuic acid against cisplatin-induced renal damage in rats. J. Funct. Foods 19, 20–27. https://doi.org/10.1016/j.jff.2015.08.028.

Zhang, T., Chen, S., Chen, L., Zhang, L., Meng, F., Sha, S., Ai, C., Tai, J., 2019. Chlorogenic Acid Ameliorates Lead-Induced Renal Damage in Mice. Biol. Trace Elem. Res. 189, 109–117. https://doi.org/10.1007/s12011-018-1508-6.